Detection of high-*Z* objects using multiple scattering of cosmic ray muons

William C. Priedhorsky,[a] Konstantin N. Borozdin, Gary E. Hogan, Christopher Morris, Alexander Saunders, Larry J. Schultz, and Margaret E. Teasdale[b]
Los Alamos National Laboratory, Los Alamos, New Mexico 87545

(Received 19 March 2003; accepted 2 July 2003)

We demonstrate that high-*Z* material can be detected and located in three dimensions using radiographs formed by cosmic-ray muons. Detection of high-*Z* material hidden inside large volume of ordinary cargo is an important and timely task given the danger associated with illegal transport of uranium and heavier elements. Existing radiography techniques are inefficient for shielded material, often expensive and involve radiation hazards, real and perceived. We recently demonstrated that radiographs can be formed using cosmic-ray muons [K. N. Borozdin *et al.*, Nature (London) **422**, 277 (2003)]. Here, we show that compact, high-*Z* objects can be detected and located in three dimensions with muon radiography. The natural flux of cosmic-ray muons [P. K. F. Grieder, *Cosmic Rays at Earth* (Elsevier, New York, 2001)], approximately 10 000 $m^{-2}\,min^{-1}$, can form useful images in ~1 min, using large-area muon detectors like those used in high-energy physics. © *2003 American Institute of Physics*. [DOI: 10.1063/1.1606536]

I. INTRODUCTION

Conventional radiography uses the absorption of man-made, penetrating radiation to provide image contrast. The flux in an image pixel is determined by Beer's law, $N = N_0 \exp(-L/L_0)$, where L is the path length through the object and L_0 is the mean free path for scattering and/or absorption.[1] The precision of radiographic measurements is limited by the Poisson counting statistics of the transmitted flux, $\Delta L/L_0 = 1/\sqrt{N}$, and the inability to penetrate dense materials. Even the most penetrating gamma rays (a few MeV) are attenuated by an *e*-folding in 2 cm of lead. Objects much thicker than this can be penetrated only by a very large incident dose, which is harmful for living organisms.

Absorption radiography has been carried out with cosmic-ray muons as well as artificial radiation. Alvarez and colleagues[2] used cosmic-ray muons to radiograph the Pyramid of Chephren in search of hidden chambers. Because of the long range of high momentum muons, this technique is only suitable for very thick objects.

II. MUON RADIOGRAPHY USING MULTIPLE SCATTERING

By contrast, our images are formed by the analysis of muon angular deflections caused by multiple Coulomb scattering. Muons undergo a random walk in direction, which yields a Gaussian angular distribution ($dN/d\Theta \propto \Theta e^{-\Theta^2/2\Theta_0^2}$), with width

$$\theta_0 = \frac{13.6\ \text{MeV}}{\beta c p}\sqrt{\frac{L}{L_0}}[1 + 0.038\ln(L/L_0)],$$

where L_0 is the radiation length, p is the particle momentum in MeV c^{-1}, and βc is its velocity.[3] The mean scattering angle is $\sqrt{\pi/2}\Theta_0$, and the rms scattering angle is $\sqrt{2}\Theta_0$. Although there are wings to this distribution, the central 98% can be described as Gaussian.[4] Since radiation length drops rapidly with atomic number, in traveling 10 cm a 3 GeV muon will scatter, on the average, 2.3 mrad in water ($L_0 = 36$ cm), 11 mrad in iron ($L_0 = 1.76$ cm), and 20 mrad in lead ($L_0 = 0.56$ cm). If the scattering angle in an object is measured, and the particle momentum is known, then the fractional path length, $R = L/L_0$, can be determined to a precision of $\Delta R/R \cong \sqrt{2/N}$, where N is the number of transmitted particles. Thus each particle delivers, via its deflection, information on the integrated radiation length along the path it traversed. In comparison, absorption radiography only contributes a binary count to a pixel.

Scattering radiography has been used in proton radiography to probe the structure and dynamics of high-density objects with accelerated high-energy protons.[5,6] While the proton technique requires large, expensive particle accelerators, the natural background of muons is free and available everywhere on the Earth. The muons are produced via interactions of primary cosmic rays in air. They are highly penetrating, having already traversed the equivalent of several meters of water by the time they reach sea level. Additionally, cosmic ray muons illuminate an object from a wide range of angles. This is helpful for three-dimensional (3D) tomographic reconstruction.

Our newly developed technique allows the study of small and medium-sized objects such as passenger cars, sea containers, and commercial trucks. Consider, for example, a truck containing normal cargo, such as a flock of sheep (40 cm thick bags of water), in which is hidden a small (10 cm thick) volume of high-*Z* material such as lead. A muon that passes through a sheep will scatter with a mean angle, θ_0, of about 5 mrad, but a muon that passes through the lead will scatter with a mean angle of about 20 mrad. By measuring

[a]Author to whom correspondence should be addressed; electronic mail: wpriedhorsky@lanl.gov
[b]Present address: University of Rhode Island, Kingston, RI 02881.

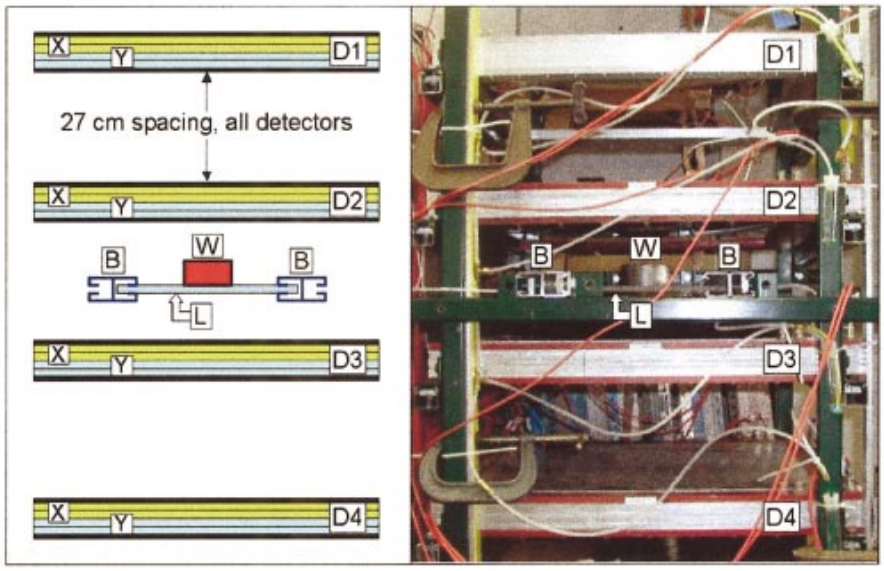

FIG. 1. (Color) The experimental apparatus. Four muon detectors (D1–D4) with a 27 cm vertical spacing were used to obtain particle positions and angles in two orthogonal coordinates (X and Y). A tungsten cylinder (W, 5.5 cm radius×5.7 cm height) was used for a test object, supported on a 1 cm thick Lexan plate (L) and steel support beams (B).

the actual scattering angles of all the muons that pass through the truck, and watching for an excess of muons that scatter through large angles, we can find the high-Z object.

To obtain a reasonable cargo screening capability, we must produce a clean detection decision in a reasonable time. Complicating factors include the clustering of muons in showers, and their distribution in momentum. The natural flux includes low momentum muons that scatter easily and high momentum muons that scatter less.

III. EXPERIMENTAL VALIDATION

To prove that these complications could be overcome, we developed a small-scale experimental detector system, which is shown in Fig. 1. The detector stack consists of four ionizing radiation tracking chambers that measure a total of eight X and eight Y locations for each muon. The active area of each delay line drift chamber detector[7] was 60×60 cm^2. The top two detectors measured the incident muon track, while the bottom two measured the track after scattering. The multiple measurements were used to resolve a directional ambiguity in drift time correction in the detectors. By calibrating of the instrument with no scattering material in the object area, we determined that our position precision was about 400 μm full width half maximum (FWHM). Data were taken using a WINDOWS® based data acquisition program developed at Los Alamos.[8] A pair of 30 cm square plastic scintillators (not shown) placed below the lowest detector were used for triggering. Given the limited acceptance angle of this configuration, the expected trigger rate was about 850 counts min^{-1}, consistent with the observed rate of 750 counts min^{-1}. A tungsten cylinder (W) of 5.5 cm radius and 5.7 cm height was used as a test object, supported by a Lexan™ plate (L) and steel support beams (B).

The path of a charged particle through the test material is stochastic and can only be approximately reconstructed. In our experiment and simulation, we used a simple technique for this reconstruction. We approximated multiply scattered tracks as having only a single scattering event, and located the point of scatter by extrapolating the incident and scattered rays to their point of closest approach (Fig. 2). The scattering signal from each muon was assigned to voxels [three-dimensional (3D) pixels] along its track using a maximum likelihood technique that distributed the signal along the track according to the uncertainty in determining the

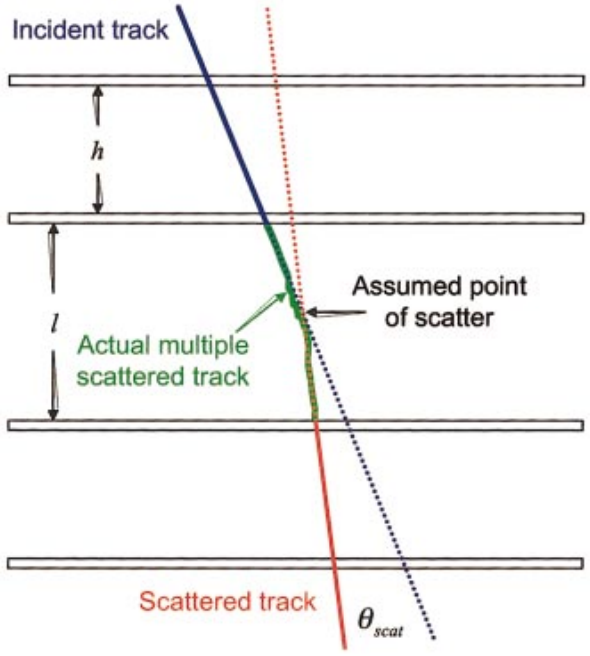

FIG. 2. (Color) Muon scattering geometry used for reconstruction. The muon trajectory is measured in four planes, two above and two below the test object. Since the incident and scattered tracks do not need to intersect (in three dimensions), the tracks are extrapolated to a point of closest approach, which is designated the scattering point. Because the scattering angles are small, most of the uncertainty in locating the point of scattering is along the track. The mean distance of closest approach increases with the thickness of the scattering material.

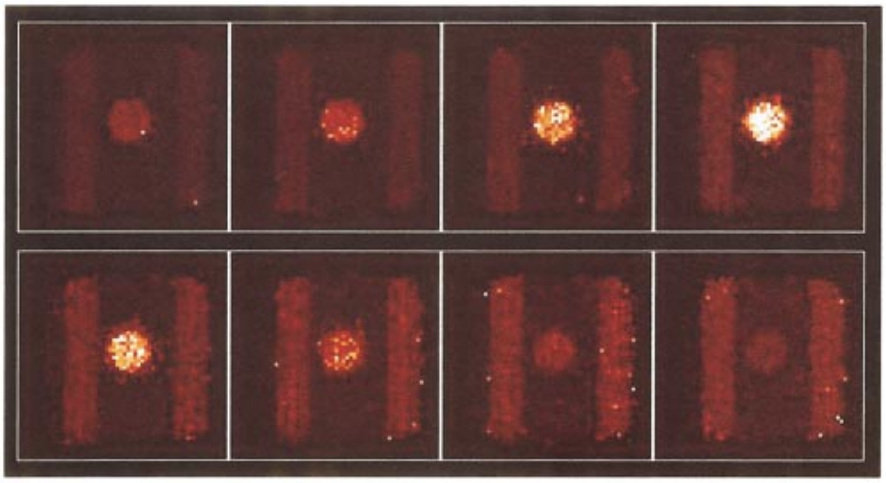

FIG. 3. (Color) Reconstruction of test object based on an experimental run of 100 000 muons. The test object is a tungsten slug 5.5 cm radius×5.7 cm height cylinder on Lexan (35×60×1 cm^3) plate with two steel rails. The reconstruction technique yields a volumetric image of 1×1×1 cm voxels; the eight planes shown are horizontal slices near the middle of the volume, moving from top to bottom. The tungsten cylinder and iron rails are clearly visible in both experiment and simulation.

point of scattering. Each scattering point was weighted by its scattering angle θ. We found that a $\theta^{1.5}$ weighting provided the highest contrast between high and low-Z objects in our images.

Figure 3 shows slices through the reconstructed, 3D image of the tungsten cylinder. The data were collected over several hours; an optimized detector with ~100% tracking efficiency and large solid angle could acquire as many muons in ~30 min. With this long run, we clearly resolve the tungsten slug, and the steel support beams as well. For a simple yes/no detection, considerably shorter runs are clearly adequate.

IV. SIMULATIONS OF LARGE OBJECTS

To compare these results with theory, and to establish a platform for investigating larger, more complex radiographic scenarios, we developed a Monte Carlo simulation code that: (i) generated cosmic ray muons with the appropriate distribution of energies and incident angles; (ii) propagated them through a test volume, calculating their scattering in each $(0.2\ cm)^3$ cubic resolution element; and (iii) generated the positions at which they would be detected in four detector planes (two above and two below the test volume). The muon spectrum, angular distribution, and rate were appropriate for sea level.[9] Their scattering and propagation within the targets were calculated according to the multiple scattering law[2] described above (e.g., assuming a Gaussian approximation). The geometry and densities of experimental test objects were incorporated in the simulation, and the same reconstruction technique used for the experimental data was applied to the simulated data. The simulation accurately matched the tungsten experiment, both in the reconstructed image, and the distribution of scatter angles.[3,10]

We used the simulation to "radiograph" larger objects than we could measure. The overall geometry is similar to our experimental setup (see Fig. 2). The detector pairs, as-

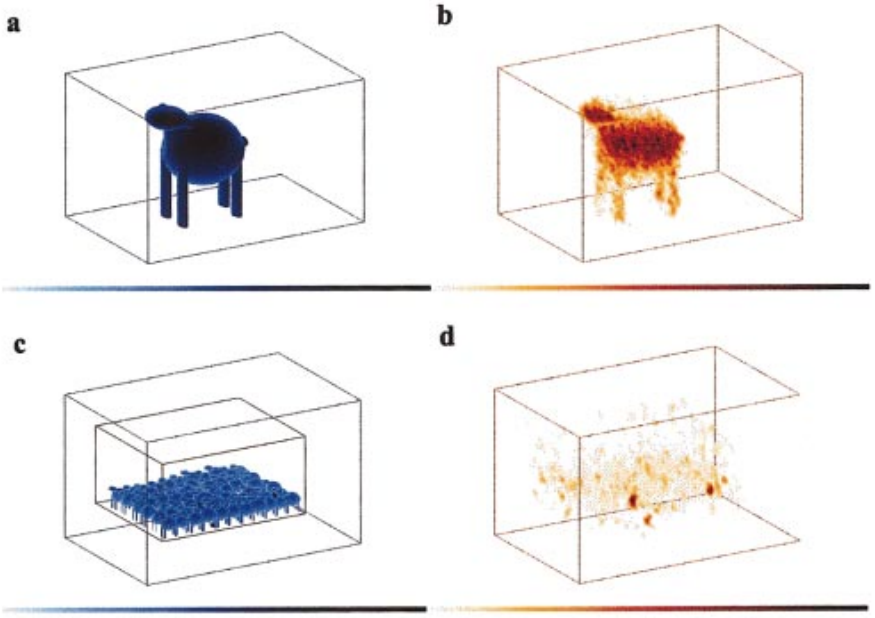

FIG. 4. (Color) Muon radiograph of a complex target, based on simulation. The test volume is 9×3×4.5 m. The first object (a) is a large lead sculpture of complex shape. The reconstructed image (b), based on 1 min of exposure of cosmic ray muon flux, shows much of the detail present in the simulated object. The second object (c) consists of a container sized at 6×2.4×2.4 m; the container walls were modeled to have a thickness equivalent to 3 mm of steel. Inside the container there are 69 "sheep" (made of water, shown in blue) each of the same complex form as the object of (a) with body sized at 60×30×40 cm^3, and three uranium bricks sized at 9×9×12 cm^3 (shown in black). The simulation represents 1 min of cosmic ray irradiation. The three "pigs" clearly stand out in the reconstructed image (d); the intensity of color in the two right panels corresponds to the significance of the signal.

sumed to have our experimental resolution of 400 μm (FWHM), are spaced 1 m apart (h) and span a 4.5 m high (l) test volume. The resolution of the image would be improved if the pairs were more widely spaced (larger h), allowing better localization of the scattering point; however, this might demand too large an instrument in a practical application. Our first target was a big lead sheep-like sculpture [Fig. 4(a)]. Reconstruction of the data simulated for one-minute exposure (using 3 cm cubic resolution elements) shows reasonably good recognition of the rather complex shape of the object [Fig. 4(b)]. We used smaller, low-Z versions of the same shape as clutter in our next simulation. The simulation modeled a steel container (3 mm walls) that contained high-Z objects (''pigs,'' the informal name for shielded casks), surrounded by dozens of low-Z objects (''sheep''). The input geometry is shown in Fig. 4(c). The ''pig'' was detected at high confidence in a 1 min simulated exposure: the signal in the $3\times3\times3$ voxel core was, in arbitrary units, 54 ± 24, while the background in an adjacent volume was 1.9 ± 1.1. This means that a threshold chosen to detect the object with 90% confidence will reject false positives from the background with 20σ confidence. Clearly, we do not expect any false positives due to statistical background fluctuations in this simulation.[11] Of course, if the surroundings are more cluttered and dense than modeled here, the background level will rise. A typical reconstruction of a 1 min simulation is shown in Fig. 4(d).

For the reconstructions shown in Figs. 4(b) and 4(d), we augmented the reconstruction algorithm, by normalizing each scattering signal by multiplying it by approximate muon momentum. An approximate knowledge of muon momentum significantly improves the signal-to-noise ratio. In the analysis above, we assumed rough knowledge of the momentum ($\Delta p/p$ of 50% in a log-normal distribution). If the momentum is unknown, our 90% threshold will reject false positives from background with 3.5σ confidence. Momentum information can be obtained inexpensively by measuring the multiple scattering in several layers of known material. This could be done by a scatter-detector sandwich that continues below the lowest detector plane. We have determined via simulation that using two planes of scattering material in this sandwich provides the needed $\Delta p/p$ of 50%. In these reconstructions, we ignore muons with momentum greater than 20 GeV c^{-1}, because the small ''scatter'' angles introduced by measurement errors appeared significant in our momentum-weighted algorithm. We also reject all rays with a scatter angle less than 5 mrad to achieve higher contrast between high-scattering and low-scattering material in the image.

V. DISCUSSION

The results so far are encouraging, and there is room for further improvement in both detection and reconstruction techniques. For instance, the displacement of the muon track (i.e., the minimum distance between the incident and scattered path) also provides a measure of multiple scattering, because multiply scattered muons are more likely to undergo a significant displacement, while a single-point scattering event necessarily has zero displacement. To achieve maximal contrast in images of different objects, one may vary weighting algorithms and apply different angular cuts.

Our results suggest, within the limitations of our model, that muon radiography of relatively large objects, on the order of the size of a commercial truck, can be performed in a reasonably short time ($\sim$1 min). The method is particularly useful in detecting a high-Z target against a low-Z background. The sensitivity of the method might be further improved by the application of a more elaborate reconstruction technique.

ACKNOWLEDGMENTS

This work was supported by the Laboratory-Directed Research and Development program at Los Alamos National Laboratory. The authors would like to thank Val Armijo and John Gomez for excellent technical support. They would also like to acknowledge Gary Blanpied of the University of South Carolina for development of the cosmic-ray muon generation software code, and John Jaros of SLAC for his thoughtful comments on the manuscript.

[1] A. Beer, Ann. Physik. Chem. **86**, 2 (1852).
[2] L. W. Alvarez *et al.*, Science **167**, 832 (1970).
[3] K. Hagiwara *et al.*, Phys. Rev. D **66**, 010001 (2002).
[4] G. R. Lynch and O. I. Dahl, Nucl. Instrum. Methods Phys. Res. B **58**, 6 (1991).
[5] N. S. P. King *et al.*, Nucl. Instrum. Methods Phys. Res. A **424**, 84 (1999).
[6] E. Hartouni and C. L. Morris, Beam Line **30**, 20 (2000).
[7] L. G. Atencio, J. F. Amann, R. L. Boudrie, and C. L. Morris, Nucl. Instrum. Methods Phys. Res. **187**, 381 (1981).
[8] G. E. Hogan, Los Alamos National Laboratory Report No. LA-UR-98-4531, 1998 ⟨http://lib-www.lanl.gov/cgi-bin/getfile?00418755.pdf⟩
[9] P. K. F. Grieder, *Cosmic Rays at Earth* (Elsevier Science, New York, 2001).
[10] K. N. Borozdin, G. E. Hogan, C. Morris, W. C. Priedhorsky, A. Saunders, L. J. Schultz, and M. E. Teasdale, Nature (London) **422**, 277 (2003).
[11] Our calculation assumes a Gaussian distribution of scattering angles, and did not consider the non-Gaussian tail of the scattering distribution. We also did not model the small fraction of cosmic rays (about 10%) which are not muons. However, low-energy electrons will be absorbed, and high-energy ($\sim$GeV) electrons behave like muons. The close accord of experiment and simulation in Ref. 1 suggests that these effects are not crucial.